FINAL PROJECT REPORT

of

Development of Heat Island Dataset for Las Vegas Urban Canopy CityGreen Analysis

Dated: February 22, 2013

Funded by:

Nevada Division of Forestry with a grant from US Forest Service

Completed by:

University of Nevada Las Vegas, Las Vegas, Nevada

PIs:

Haroon Stephen (*Civil and Environmental Engineering*)

Craig Palmer (*Harry Reid Center for Environmental Studies*)

Sajjad Ahmad (*Civil and Environmental Engineering*)

Graduate Student:

Adam Black

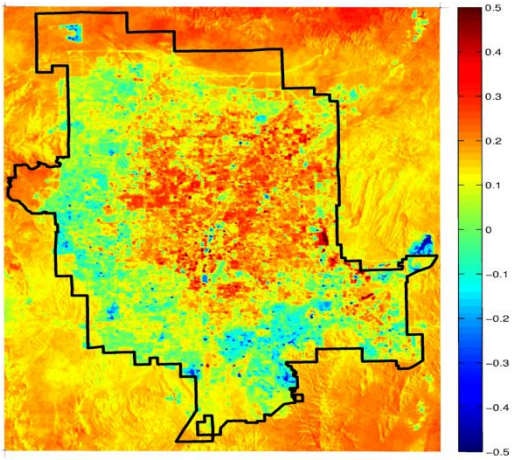

This project is funded through grants from the US Forest Service. NDF and USFS are equal opportunity service providers. "In accordance with Federal law and U.S. Department of Agriculture policy, this institution is prohibited from discriminating on the basis of race, color, national origin, sex, age or disability. (Not all prohibited bases apply to all programs.)

To file a complaint of discrimination: write USDA, Director, Office of Civil Rights, Room 326-W, Whitten Building, 1400 Independence Avenue, SW, Washington, D.C. 20250-9410 or call (202) 720-5964 (voice and TDD). USDA is an equal opportunity provider and employer."

Executive Summary

Las Vegas has almost doubled its population during the last two decades and undergone exponential urban sprawl. The urban growth brings about changes that adversely impact the quality of urban life. The urban heat island (UHI) effect is a common problem of present day growing cities. In order to take measures for UHI reduction, it is imperative that the UHI hotspots are mapped and related to landcover characteristics.

This document is the final report of project "*Development of Heat Island Dataset for Las Vegas Urban Canopy CityGreen Analysis*" funded by Nevada Division of Forestry. The report provides analysis of the landcover maps, urban/suburban boundaries, urban zoning data, remote sensing data, and meteorological data to identify the urban heat islands in Las Vegas Valley.

Ground based measurements from Weather Underground stations provide air temperature. The air temperature trends show decreasing trends at most of the points. This trend is especially seen in the areas of new development where the age of measuring station is less than 10 years. Nevertheless, the older meteorological stations show positive temperature trends possibly linked to long term climate change effects. Similar analysis of remote sensing thermal imagery provides better spatial perspective of the situation. Although remote sensing temperature data corresponds to the surface and not air, it corroborates the general trends seen in ground measurements. It provides additional insight regarding the impact of new development on the temperature trends. It is observed that the new development during the last two decades show sustained temperatures rather in some cases show decreasing trends. This effect is evident in the fringe of Las Vegas city that was developed in last two decades.

In order to measure the urban heat island effect, urban heat island intensity (UHII) is measured as a difference of midnight and noon temperature. It is based on the observation that the urban heat islands that retain heat during the night do not cool down sufficiently and thus have temperatures closer to noon temperatures. Since midnight and noon temperature data of the whole valley is not available, it is estimated by developing regression relations between ground measurements and remote sensing thermal images. High UHII values indicate potential urban heat island and are observed at the airport and in the industrial areas. The results provide useful insight into the temporal thermal behavior of Las Vegas area.

Table of Contents

Table of Figures

1 Introduction

Las Vegas has grown significantly from a small city incorporated in 1911 to the most populous city in the State of Nevada. Being an attractive entertainment destination, Las Vegas attracts millions of tourists and part-time workers every year. Moreover, being a semi-arid warm region, it has also been a popular retirement destination. Thus, Las Vegas has almost doubled its population during the last two decades and undergone exponential urban sprawl. The urban growth brings about changes that adversely impact the quality of urban life. The urban heat island (UHI) effect is a common problem of present day growing cities. In order to take measures for UHI reduction, it is imperative that the UHI hotspots are mapped and related to landcover characteristics.

This document is the final report of project "*Development of Heat Island Dataset for Las Vegas Urban Canopy CityGreen Analysis*" funded by Nevada Division of Forestry. The report provides analysis of the landcover maps, urban/suburban boundaries, urban zoning data, remote sensing data, and meteorological data to identify the urban heat islands in Las Vegas Valley. The overarching goal of the project is to facilitate identification of potential areas for planting trees in the valley to reduce in the heat island effect.

This report is organized as follows. Section 2 provides background information about the urban heat island effect. It is followed by a description of the study area and data in Section 3. Section 4 describes the time series and trend analysis using ground based temperatures data which is followed by a similar analysis of remote sensing based temperature in Section 5. Section 6 described UHII mapping using a regression model of remote sensing and ground based temperature data. Section 7 describes the preparation of an integrated landuse map of the valley. Section 8 provides a summary and conclusions.

2 Urban Heat Island Effect

Urban heat island effect is a phenomenon where temperature in cities is higher than in surrounding rural areas. UHI is caused by high absorption of heat energy by urban materials (asphalt, concrete, roofs tiles) and entrapment of this energy due to nighttime inversion from stabilization of the urban boundary layer (*Chen et al., 2011; Bornstein, 2009*). UHI has adverse impacts on quality of life such as health problems (*Frumkin, 2002*), a rise in urban water and energy demands (*Guhathakurta and Gober, 2007; Kolokotroni et al., 2006*), and impaired ecosystems in surrounding water bodies by warm water discharge from cities (*Imhoff, 2012*). UHI also has adverse impacts on local meteorology such as altered wind patterns, humidity, clouds, and precipitation (*Grimmond and Oke, 2002*).

Urban heat island intensity (UHII) is the difference between urban temperature and a base rural temperature and is a metric used to quantify the thermal impact of urban development (*Arnfield, 2003*). UHII is related to city size (*Oke, 1973*), urban population (*Oke, 1976*), and urban landuse practices (*Chen, 2006*). UHII varies with time of day and year and values as high as 10°C (18°F) have been reported (*Carlowicz, 2009; Remar 2010*). Urban population continues to increase stimulating more development and landuse change in cities. Thus, it is imperative to relate the landuse change practices and subsequent response of UHII. Las Vegas's population and size has almost doubled in the last decade (*City Council Report, 2010*) and this rapid growth provides an opportunity to understand the dependence of UHII on landuse practices and find its response to landuse change (*Xian and Crane, 2006; Remar, 2010*).

An urban heat island is caused by shifting local thermal equilibrium due to altered surface absorption and emission characteristics. It is caused by urban growth i.e., lateral expansion as well as upward rise of the urban skyline. With the expansion of urban boundary, natural landscape is converted into urban landscape consisting of high specific heat material (asphalt and concrete). Moreover, with the rise of the urban skyline, valleys and canyons are created that have reduced air exchange with the atmosphere above the skyline. Thus, both lateral expansion and upward rise result in increased temperatures in dense urban areas resulting in urban heat island effect.

In order to understand the urban heat island effect, it is important to understand the thermal process in the natural environment. All thermal processes are primarily energized by the solar energy and regulated by the natural environment. In the natural environment, the typical constituents of the landscape are rock, soil, water, and vegetation. These constituents respond to solar energy reflection/scattering, transmission, absorption, emission, and metamorphosis. These processes are explained as follows:

Reflection/Scattering is the process where incident energy is reflected back due to the surface reflectivity characteristics and returns into the atmosphere contributing to Earth's albedo.

Transmission is passing-through of the incident energy through the intervening medium where it undergoes volume absorption and scattering. The energy may reach the next layer and undergo another round of absorption/reflection.

Absorption is the process where incident solar energy is absorbed and becomes part of the internal energy of the medium. This is governed by the absorptivity characteristics of the material.

Emission/Re-radiation is the energy emitted back into the atmosphere. In thermal equilibrium, absorption is equal to emission. If absorption is greater than emission, the body's temperature increases and *vice versa*. This is governed by the emissivity characteristic of the material.

Metamorphosis is conversion of incident energy into chemical energy (photosynthesis), mechanical energy (weathering), or electric energy (photoelectric effect).

The net thermal effect of these processes is heating and cooling cycle of the material which is synchronous with the diurnal behavior of solar energy. When the natural terrain is converted into urban terrain, the processes remain the same but the intensity and rates are changed. For example, due to the new materials introduced in the area (concrete, asphalt), the emissive, absorptive, and reflective characteristics change leading to following effects:

1. shift of the thermal equilibrium.
2. energy retention due to high specific heat materials
3. energy entrapment in urban canyons between large buildings
4. overheating or overcooling, and
5. shifts in the diurnal cycle.

These effects lead to creation of urban heat islands or urban cool islands. UHI are the neighborhoods where the area doesn't cool down at night due to blockage at night of the escape routes of the heat energy that was absorbed during the day. Urban cool islands are the areas where the energy intake routes are blocked during the day and it doesn't receive sufficient energy during the day. Either way the thermal equilibrium is shifted to a new balance point.

Although the shift in the thermal equilibrium is a natural process, it affects life. In the natural environment, the shifts in the thermal equilibrium are slow and are accompanied by species migrations, species phonological changes etc. The shifts in the urban thermal equilibrium are drastic and thus have devastating effects on the human population as well as on the other life forms. Some of the known issues are 1) health issues (heat stroke), 2) energy demand (AC/heaters), 3) water demand (cooling), and 4) air quality (haze/inversion).

There is a great interest in determining the urban configurations that would eradicate and prevent urban heat islands. Masson has provided a review and classification of urban surface energy balance models and their applicability based on scale of study, focus of interest, and observational data availability. It is indicated that urban material modification could be a potential research direction to mitigate urban heat island. (Mason, 2006). Increasing canopy cover by planting trees is a common practice adopted by many cities. This research is conducted

to identify urban heat islands in Las Vegas to facilitate and focus tree planting efforts by the Nevada Division of Forestry.

Spaceborne thermal remote sensing techniques have been developed and successfully applied to map UHI in various urban areas (*Voogt and Oke, 2003; Xian and Crane, 2006*). Thermal remote sensing data can be used to study the differnce between midnight and noon temperature measurements of Las Vegas. In this research, we use ground measurements of air temperature and remote sensing measurements of lands surface temperature to analyze the spatio-temporal thermal behavior of Las Vegas urban area. Ground based temperature measurements are used to perform trend analysis of temperature time series. Statistical relationships are developed between air temperature and land surface temperature that are used to estimate the midnight and noon temperature from the remotely sensed temperature data. Since urban heat islands have high nighttime temperature, we define urban heat island intensity as the difference between the midnight and noon temperature. Spatial estimates of UHII are mapped and used to identify the urban heat islands. Landuse and tree canopy maps of Las Vegas are used for comparison in this analysis.

3 Study Area and Data

This section provides brief information about Las Vegas followed by description of data used in this research.

3.1 Las Vegas Urban Area

Study area includes the greater Las Vegas metropolis which includes City of Henderson, City of Las Vegas, City of North Las Vegas, and unincorporated Clark County intervening areas contained within the Bureau of Land Management (BLM) disposal boundary. Las Vegas is a Spanish word meaning “the meadows” or “fertile lowlands”. This name refers to the natural springs charged by an expansive aquifer that covers a majority of the valley. This reliable water source became a popular stopping point for travelers heading towards Los Angeles or for settlers seeking to farm or work in nearby mines between 1850 and 1900. On May 15, 1905, 110 acres was auctioned off establishing Las Vegas city area. City government was established by 1911 with a city population just over 800 people. City expansion steadily grew to 5,165 residents by 1930. Completion of Boulder Dam in 1935, establishment of industrial and military complexes during WWII in the 1940’s, and Las Vegas’ notoriety as an entertainment capitol led to, on average, an accelerated population growth rate of approximately 7% per year between 1910 and 2000. This population boom introduced heavy urban development and expansion. The population over the last 20 years has more than doubled (Figure 1). This rapid increase has resulted in major conversion of natural surfaces to urban landscape and altered the

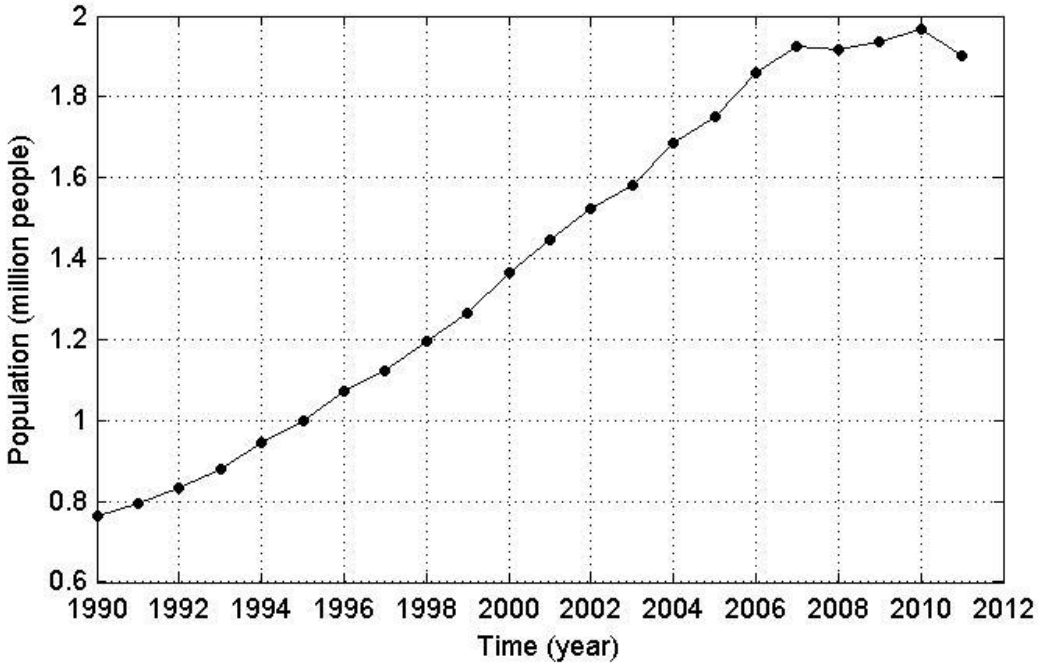

Figure 1. Time series of the population of Las Vegas urban area. (Data source: Clark County Department of Comprehensive Planning, SNRPC Consensus Population Estimate.)

thermographic, hydrographic, and orographic behavior of the landscape. Figure 2 shows that change in the urban footprint through comparison of 1984 and 2009 LandSat true color composite images. Las Vegas urban footprint has significantly stretched during the last 3 decades. Although the city didn't expand much towards east due to the natural barrier from Frenchman mountain, the city has grown almost equally in all other three directions. The change in the landscape has occurred in two ways. Firstly, surface characteristics have changed including a reduction in desert and open surface, increase in anthropogenic materials (asphalt, concrete, etc.), increase in urban sprawl with more housing density, exogenous vegetated surfaces, altered surface elevation, altered surface roughness, and landscape fragmentation due to roads. Secondly, natural processes have changed including life processes (desert flora and fauna) disturbance, hydrographic response change, orographic response change, and thermal response change causing urban heat or cool islands.

3.2 Data

The data for this research includes zoning maps from various cities of Las Vegas metropolis, meteorological data from weather underground stations, and thermal remote sensing data from LandSat 5 Thematic Mapper imagery. These data sets are described as follows.

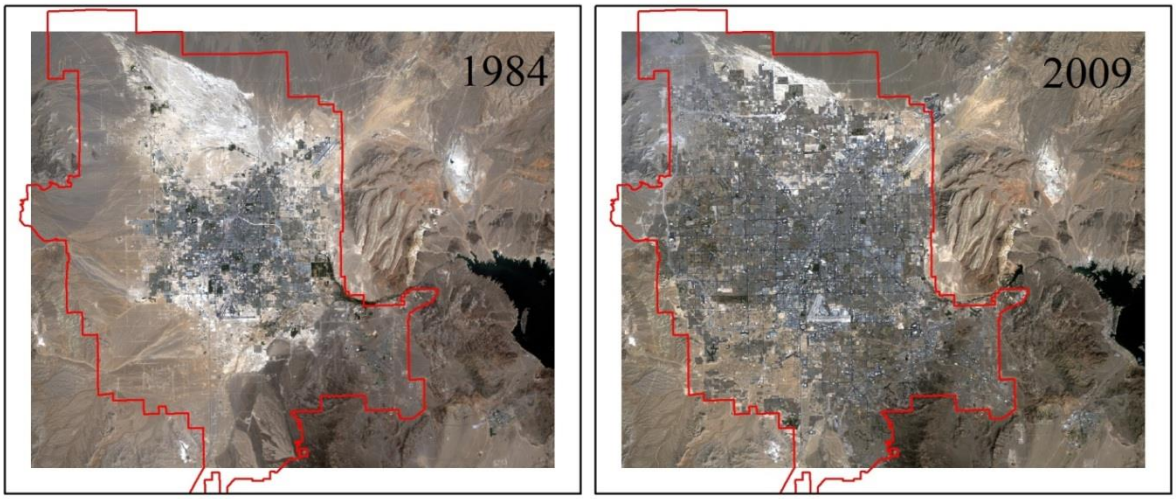

Figure 2. Las Vegas urban change between 1984 and 2009 as viewed by LandSat 5 Thematic Mapper. Las Vegas disposal boundary polygon is overlaid for reference.

3.2.1 Planned Landuse Data

Las Vegas valley zoning map of the planned landuse is prepared by merging the land use boundaries and government zones across all the cities. Each city has developed a zoning map with custom building codes of landuse characteristics. These maps were merged to create a unified landuse map of Las Vegas. GIS layers of the zoning maps were accessible at the Clark County GIS Management Office (GISMO) website (*GISMO, 2012*). The data used for preparing the zoning map is listed below.

City of Henderson

Existing Zoning map by Geographic Information Services created Sept. 2011.

HDZoning shapefile by Community Development GIS adopted July 20, 2010.

City of Las Vegas

City of Las Vegas Zoning map by Planning & Development Dept. created July 11, 2011.

CLV_Zoning shapefile – File description does not include publisher and date within metadata information.

City of North Las Vegas

Zoning map by Community Development Dept. Planning and Zoning Division GIS Services created March 31, 2011

NLVZONE_P shapefile – File description does not include publisher and date within metadata information.

Clark County (Material created by Comprehensive Planning Dept.)

Enterprise Planning Area map created Nov. 4, 2009
CC_ENTPLU_p shapefile created Sept. 2, 2009
Lone Mountain Planned Land Use map created Oct. 14, 2008
CC_LMPLU_p shapefile created Sept. 17, 2008
Northeast County Planned Land Use map created Oct. 4 2006
CC_NEPLU_p shapefile created Sept. 6, 2006
Northwest County Planned Land Use map created April 10, 2008
CC_NWPLU_p shapefile created Nov. 7, 2007
South County Planned Land Use map created Feb. 8, 2007
CC_SCPLU_p shapefile created Dec. 6, 1994
Spring Valley Planning Area map created Nov 4, 2009
CC_SPVPLU_p shapefile created Dec. 10 2004
Sunrise Manor Planning Area map created Oct. 11 2010
CC_SRMPLU_p shapefile created Jan. 18, 2006
Summerlin South Planned Land Use map created April 18, 2007
CC_SUMPLU_p shapefile created May 28, 2003
Whitney Planned Land Use map created May 15, 2007
CC_WHPLU_p shapefile March 21, 2007
Winchester and Paradise Planned Land Use map created Sept. 8, 2010
CC_WPPLU_p shapefile created Aug. 3, 2005

3.2.2 Meteorological Data

Meteorological data for this research was acquired primarily from Weather Underground (WUnderground) Network. Data from weather stations at the airports and air force base was also used. WUnderground is a name coined for Weather Underground project which is a network of privately owned meteorological sensors installed in home backyards and connected to the Internet. A central server system continuously receives and archives data from the WUnderground stations and displayed on the WUnderground website (*Wunderground 2013*).

WUnderground network project was started in the Fall of 1995 and provides weather forecasts, current weather conditions, and hourly data for over 550 US cities. It has grown to be the largest personal weather station (PWS) network of approximately 36,000 stations with almost 23,000 located in the US. Although WUnderground does not provide certified weather data, strict quality controls are applied to these meteorological stations. Temperature observations at PWS are recorded approximately every 15 minutes. The website also hosts weather information

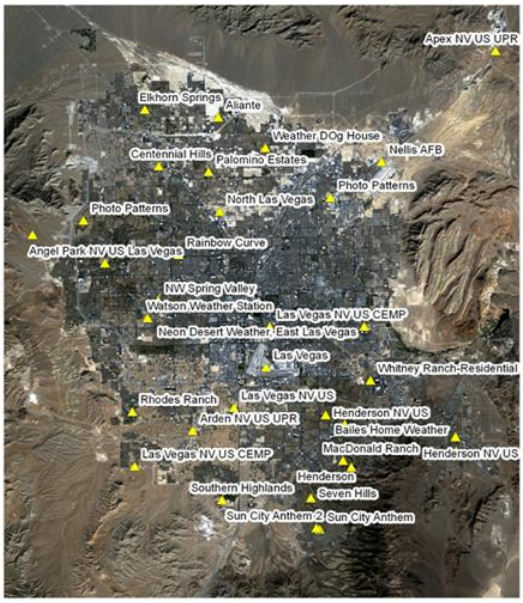

Figure 3. Las Vegas study area and meteorological station locations.

from other systems such as Airport Automated Surface Observation Systems, the Meteorological Assimilation Data Ingest System, and the National Oceanic and Atmospheric Administration. Weather conditions for these stations are reported on an hourly and sub-hourly basis. In this project, temperature records are used from 23 wunderground PWS, 4 airport monitored weather stations, and 3 community environment monitoring programs. The meteorological station locations and study area are identified in Figure 3.

3.2.3 LandSat 5 Thematic Mapper Thermal Infrared Imagery

The Landsat program is a long term corroborative effort between the U.S. Geological Survey (USGS) and the National Aeronautics and Space Administration (NASA) to gather satellite remotely sensed spectral images of the Earth's surface. LandSat has been one of the most successful Earth observation missions. LandSat provides almost 30 years of uninterrupted time series of global optical and thermal remote sensing data (*USGS Global Visualization Viewer, 2012*).

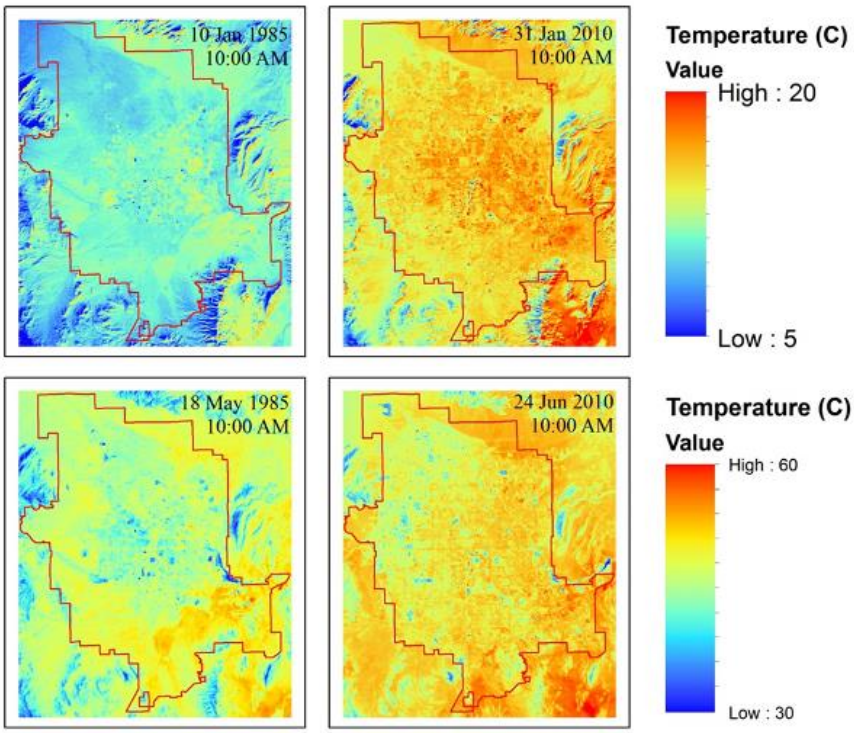

Figure 4. Comparison of LandSat 5 TM thermal infrared imagery during 1985 (left column) and 2010 (right column). Winter (top row) and late spring/early summer (bottom row) comparison is shown.

Thematic Mapper (TM) is a 7 band instrument aboard LandSat 5 mission where each band tracks the reflected radiance of a surface within a portion of visible, infrared or thermal infrared spectrum. Thematic Mapper measures thermal infrared radiance between wavelength range 10.4 to 12.5 µm called band 6. Thermal infrared band has a spatial resolution of 120 meters and can be used to estimate the land surface temperature. We use thermal infrared data between May 1984 and November 2011 over Las Vegas to map the land surface temperature. This comprises of approximately 360 remote sensed images where each image corresponds to 10:00 am and 11:00 am Pacific Standard Time (PST) when Landsat 5 satellite passes over the Las Vegas Valley area. Figure 4 shows a comparison of land surface temperature during 1985 and 2010 for winter and late spring. The January image of 2010 shows significantly higher temperatures compared to 1985 image. Somewhat lesser but similar behavior is observed in the late spring images. Although this indicate warming in 2010 but it doesn't confirm any trend as these images are represent a snap shots in time. In later analysis, it is shown that trends do exist that are revealed through results of time series analysis.

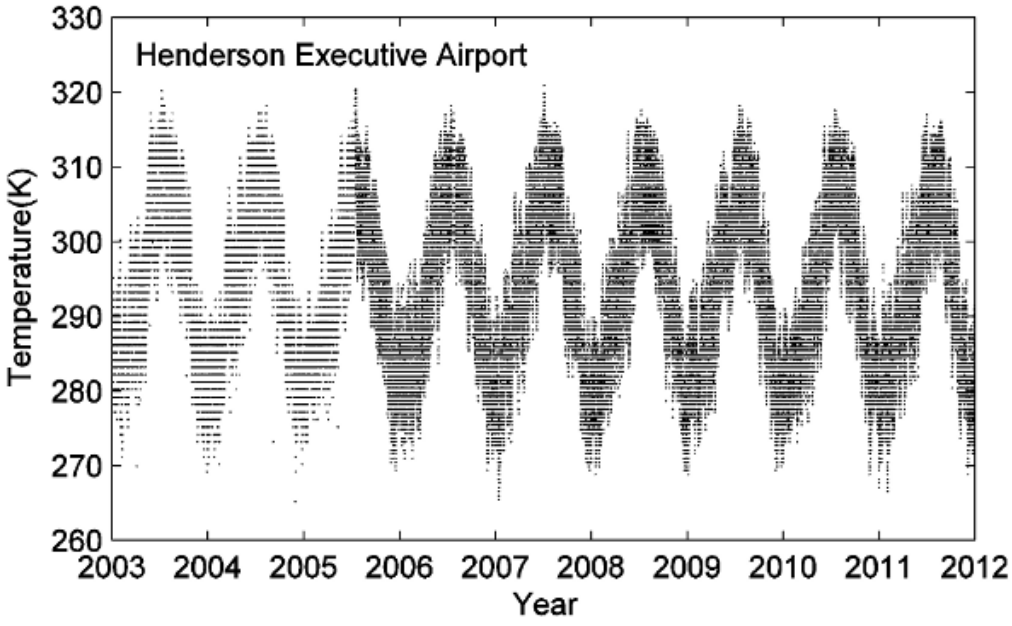

Figure 5. Temperature time series of meteorological station at Henderson Executive Airport.

4 Temperature Trend Analysis of WUnderground Data

In this section, the trend analysis of the point temperature measurements from WUnderground stations is presented. The temperature temporal variation is used to understand the evolution of the surface thermal behavior. Although the process is shown for a selected station at Henderson Executive Airport, the results are calculated and tabulated for each meteorological station. Figure 6 shows the multi-annual temporal variation of temperature at the selected station. A careful observation shows long term trend of reducing temperature. Generally, it is difficult to estimate the long term trend in the presence of the annual cycle. Thus, an anomaly analysis is performed where annual cycle at each station is removed from the time series.

In the anomaly analysis, the average annual temperature response is calculated through the multi-year average of temperature for each day of year. Figure 7 shows such response for the selected station which is typical for the Las Vegas area. Residual temperature is defined as the deviation of the temperature on a given day from the multi-year average temperature value of that day. Figure 8 illustrates the time series of the residual temperature at the selected station showing better clarity of trend compared to Figure 6.

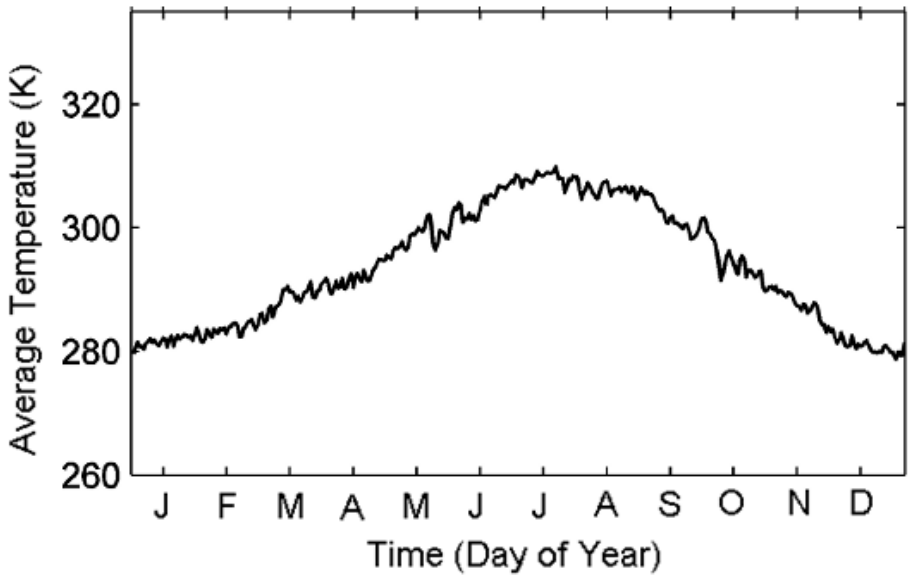

Figure 6. Average annual temperature response calculated for meteorological station.

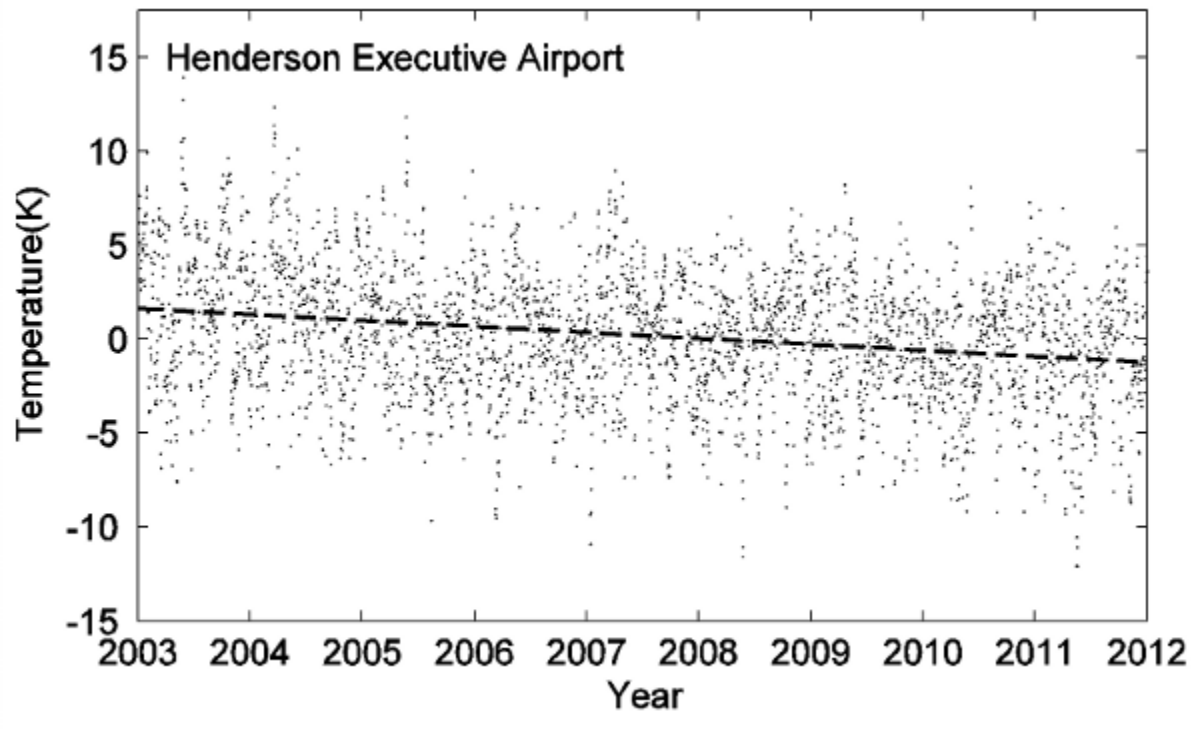

Figure 7. Residual temperature time series calculated by subtracting the average annual response.

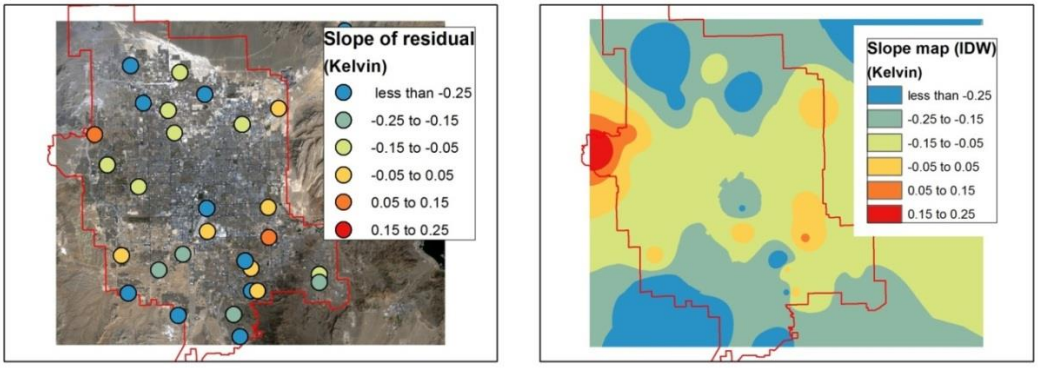

Figure 8. (Left) LandSat image overlaid with color coded values of temperature trend. (Right) Spatial map of temperature trend created by Inverse Distance Weighted (IDW) interpolation of point data.

The dashed line in Figure 8 plot is a least squared fit to the residual time series data. It is evident from the slope of the line that temperature is decreasing with a rate of 0.32 K/year. The slope of the residual temperature was computed for all the WUnderground stations and in general most stations show trends of decreasing temperature as shown in table in Appendix A. The time range of input data is also shown which reflects the temporal domain of the calculated trend. The stations that were installed during the last decade show a decreasing trend whereas the stations with multi-decadal data show a positive trend. This indicates that although there is long term warming or Las Vegas, there are cooling trends during the last decade. In order to better understand the spatial patterns Figure 9 (left) shows color coded points. Note that positive temperature trends occur at McCarran airport, Photo Patterns, and Summerlin West NV stations. Since Summerlin West NV station only has data for two years this trend only applies to 2010-2011 period.

Since the trends are based on specific point data, spatial interpolation is performed to estimate the trends in other parts of the city. Inverse Distance Weighted (IDW) interpolation is performed and the results are plotted in Figure 9. It is noted that the confidence in the interpolated values decreases away from the locations of input data. Nevertheless, it shows the spatial patterns otherwise not available due to lack of sufficient ground measurements. Figure 9 (right) shows that there is no significant temperature trend in the central Las Vegas. Some areas show increasing trend and correspond to the airport and the industrial areas in Las Vegas. Moreover, the north and south area shows decreasing trends. The trend analysis provides meaningful insight that is further explored using the LandSat thermal imagery. This analysis is described in the next Section.

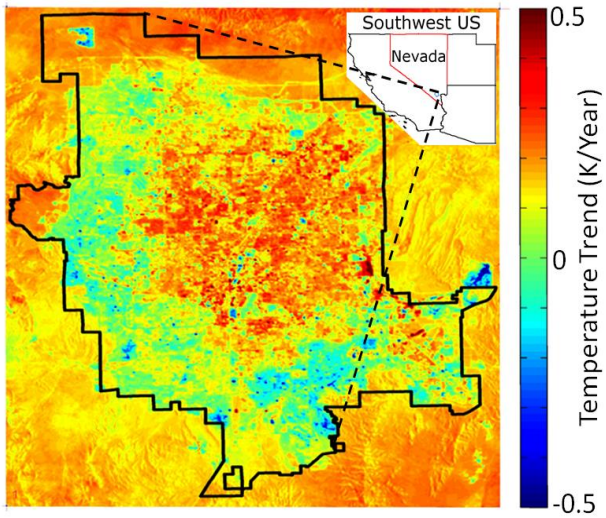

Figure 9. Spatial map of temperature trend estimated from LandSat TM 1990-2010 data.

5 Temperature Trend Analysis of LandSat Thematic Mapper Temperature Data

The previous analysis was based on point measurements. In order to confirm these results and get a better spatial understanding of the trends, we also conducted trend analysis using LandSat Thematic Mapper derived temperature data. Similar procedure as described in Section 4 is used where mean annual response was subtracted to find residual temperature and slope of regression line was computed to estimate trend. This was performed for each pixel of LandSat TM image. Figure 9 shows the spatial map of the slope of residual temperature. This map illustrates that the old Las Vegas urban and rural area have continued to increase in surface temperature due to general climate trends but the new development area in the fringe of the Las Vegas city does not show increasing trends. It is noted that in general the new development area has higher tree canopy cover.

It is noted that the analysis of Section 4 corresponds to air temperature where as Figure 9 corresponds to the surface temperature. These two analyses provide different views of the urban heat island effect that surface level and canopy level.

6 UHII from Regression Model of Wunderground and LandSat Temperature

This section describes the analysis performed to estimate temperature trends from the LandSat thermal remote sensing data and to create a map of urban heat island intensity. Firstly, the process of converting LandSat band 6 digital numbers to land surface temperature is shown.

Thermal infrared remote sensed data is converted to land surface temperatures (LST) in Kelvin units using the inverse of Planck's Theorem stated as

$$LST = \frac{K_2}{ln\left(\frac{K_1 \cdot \varepsilon}{L_\lambda} + 1\right)} \quad (1)$$

where K_1 and K_2 are parameters adjusting for equipment bias. Emissivity, ε, accounts for atmospheric interference which is general set as 0.95. L_λ is the spectral radiance calculated from the digital number value of the raster image using the gain and offset values of the thermal infrared band (National Aeronautics and Space Administration, 2008). Figure 10 shows the time series of WUnderground temperature (WUT) and LST at a selected station. Note that LST is in general higher than WUT as would be expected since WUT reflects the air temperature and LST is the surface temperature.

The LST temporal resolution is coarse compared to WUT data but its spatial resolution is much finer compared to point based WUT data. Thus, we devised a technique to infer LST from the WUT. This technique is based on developing a linear relationship between the two values. As indicated earlier, the urban heat islands are areas where the night time temperature stays high due to the heat entrapment. Thus, it is hypothesized that the difference between the noon and midnight temperature at a given point is an indicator of its urban heat island intensity. Figure 11 shows the diurnal variation of the WUT data which clearly shows the lowest point around sunrise and a peak in the afternoon.

We develop relationships between LST and WUT at midnight ($WUT_{midnight}$) and at noon (WUT_{noon}) using the historical data at all WUnderground stations. The models are given by

$$WUT_{midnight} = A_m \, \mathrm{LST} + B_m \quad (2)$$

$$WUT_{noon} = A_n \, \mathrm{LST} + B_n \quad (3)$$

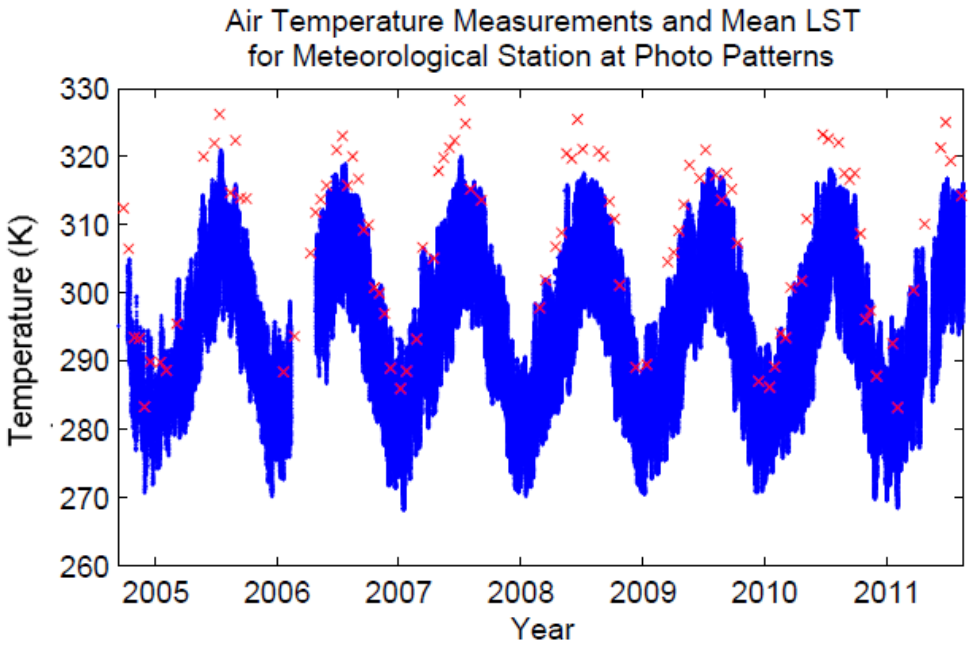

Figure 10. Graph showing a multi-year time series of air temperature observations (blue dots) from WUnderground station at Photo Patterns station (ID: KNVLASVE23). The corresponding 500 m buffer average land surface temperature (red crosses) from LandSat thermal imagery is also shown.

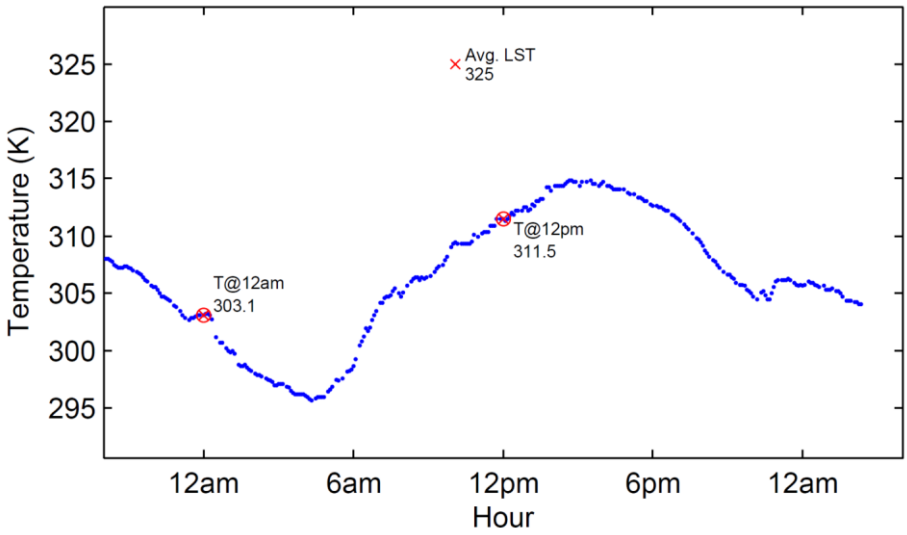

Figure 11. Graph showing typical diurnal variation of air temperature observations (blue dots) from WUnderground station at Photo Patterns station (ID: KNVLASVE23). The midnight and noon temperatures (red circles) are also indicated and corresponding 500 m buffer average land surface temperature (red crosses) from LandSat thermal imagery at 10AM is shown as well.

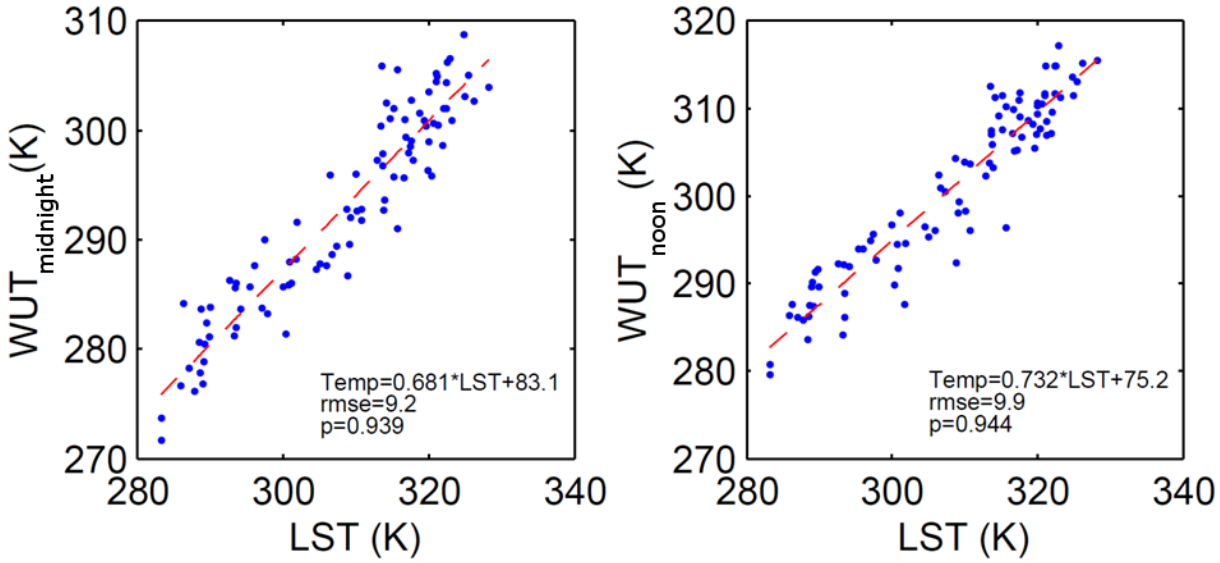

Figure 12. Graph showing relationships between average land surface temperature from LandSat thermal imagery and (a) midnight air temperature and (b) noon air temperature observed at WUnderground station Photo Patterns.

where A_m and B_m are parameters for midnight linear relationship and A_n and B_n are parameters for noon linear relationship. Figure 12 graphically demonstrates relationships at the Photo Patterns station. The model equations are also written in the figure. Model parameters are calculated for all the WUnderground stations and listed in Appendix B. Since these parameters reflect the relationship between WUT and LST, if available at each point these can be used to estimate WUT over the whole study area. We use IDW interpolation to compute the model parameters everywhere in the region depicted in Figure 13. The images of the model parameters show spatial coherence related to the urban thermal response. These images are used to compute the midnight and noon WUT values that reflect the spatial distribution of the air temperature.

Using the LandSat thermal infrared image on August 30, 2011 WUT images of midnight and noon are calculated and shown in Figure 14. In general, the difference between night and day time temperature values is obvious showing relatively cooler night temperature. Moreover, these images also show the spatial variations that are dependent upon the urban layout as can be seen if compared to the LandSat optical image in Figure 3. As hypothesized earlier, the difference between noon and midnight air temperature is related to the urban heat island effect.

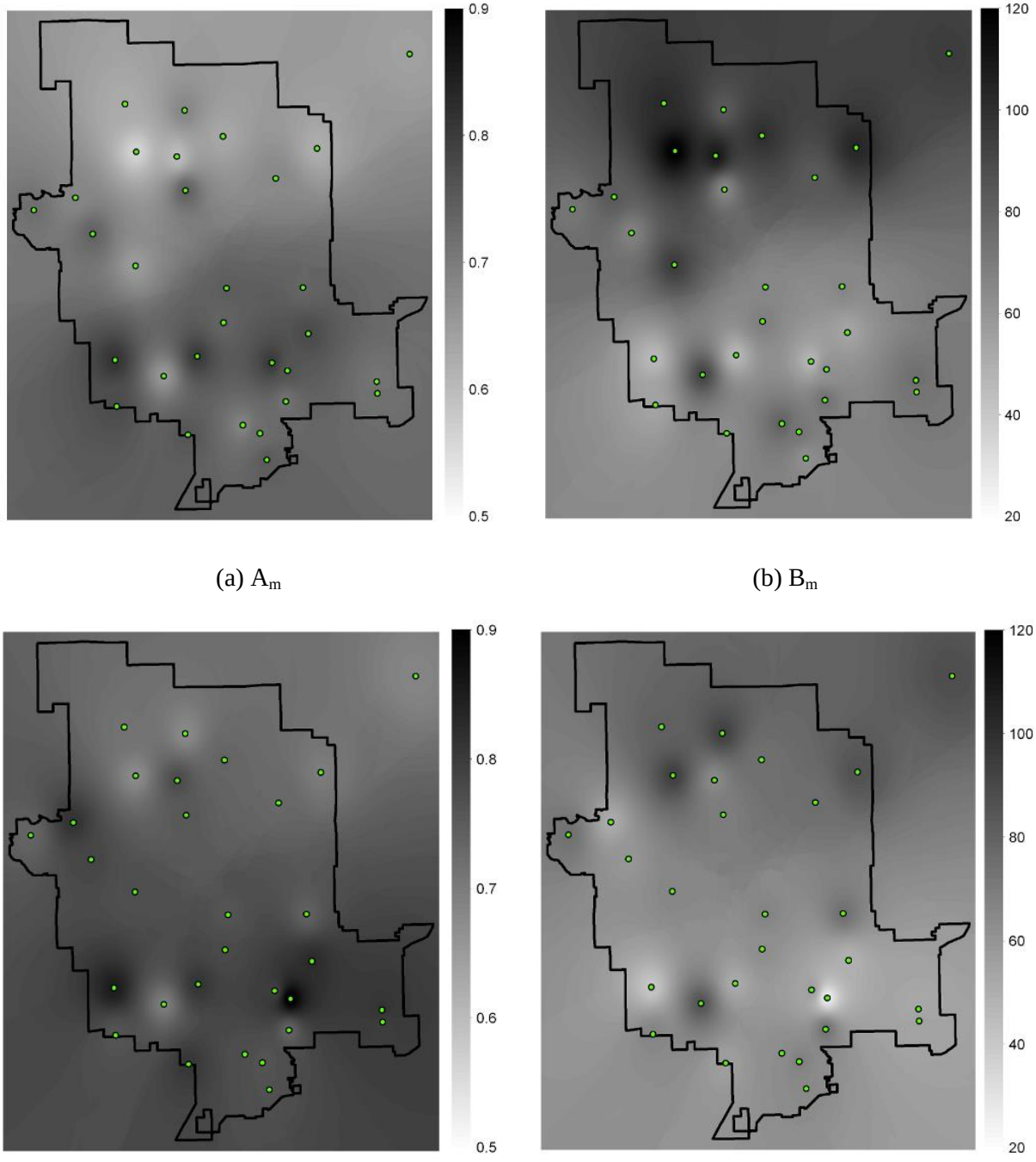

(a) A_m (b) B_m

(c) A_n (d) B_n

Figure 13. Images of linear model parameters for midnight [(a) and (b)], and noon [(c) and (d)].

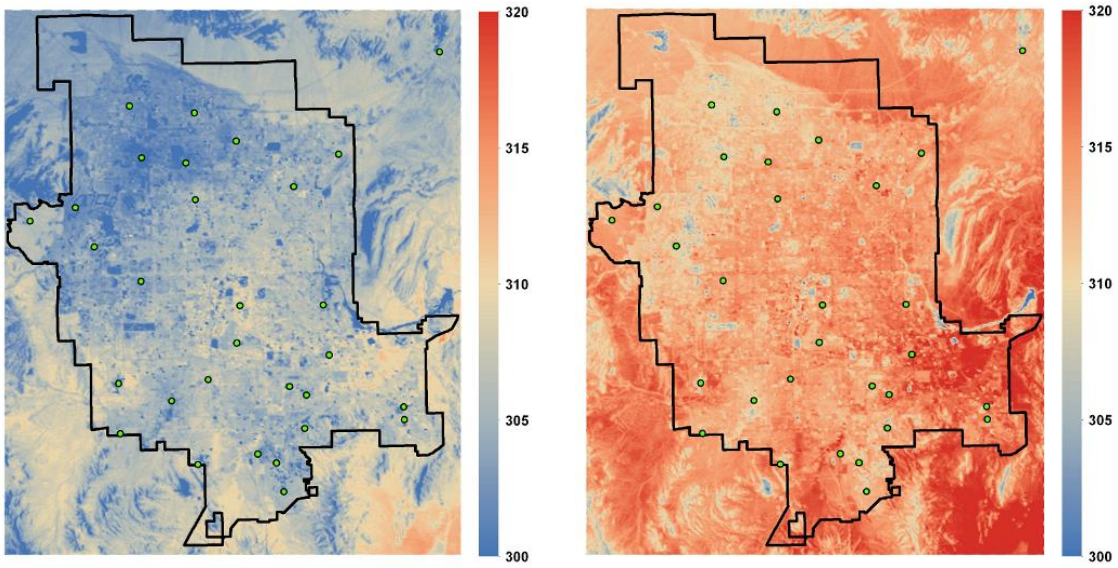

Figure 14. Images of estimated midnight (left) and noon (right) air temperature for June 27, 2011.

We define urban heat island intensity (UHII) as

$$UHII = \mathrm{WUT}_{\mathrm{midnight}} - \mathrm{WUT}_{\mathrm{noon}} \tag{4}$$

where lower values of UHII indicate an urban heat island.

Figure 15 (top) shows the map of UHII computed from August 30, 2011 LandSat thermal imagery. Note that UHII is a negative number. UHII = 0 is the extreme case where the incoming energy is permanently trapped and midnight temperature is equal to the noon temperature. As the UHII becomes negative (reduces), that indicates greater difference between midnight and noon temperature. It is seen that highest values of UHII = -5 are observed in several parts of the city. These areas mainly correspond to the airport, industrial areas, and older parts of the city. The newer developments, generally, have values less than -8.

In Figure15, comparing UHII map with Landsat true color image reveals that urban regions with minimal temperature variation of UHII between -8.5 and -7 are located south of Tropicana Road and west of Green Valley Parkway / US Route 95. This area largely consists of undeveloped land with undetectable presence of landscape vegetation.

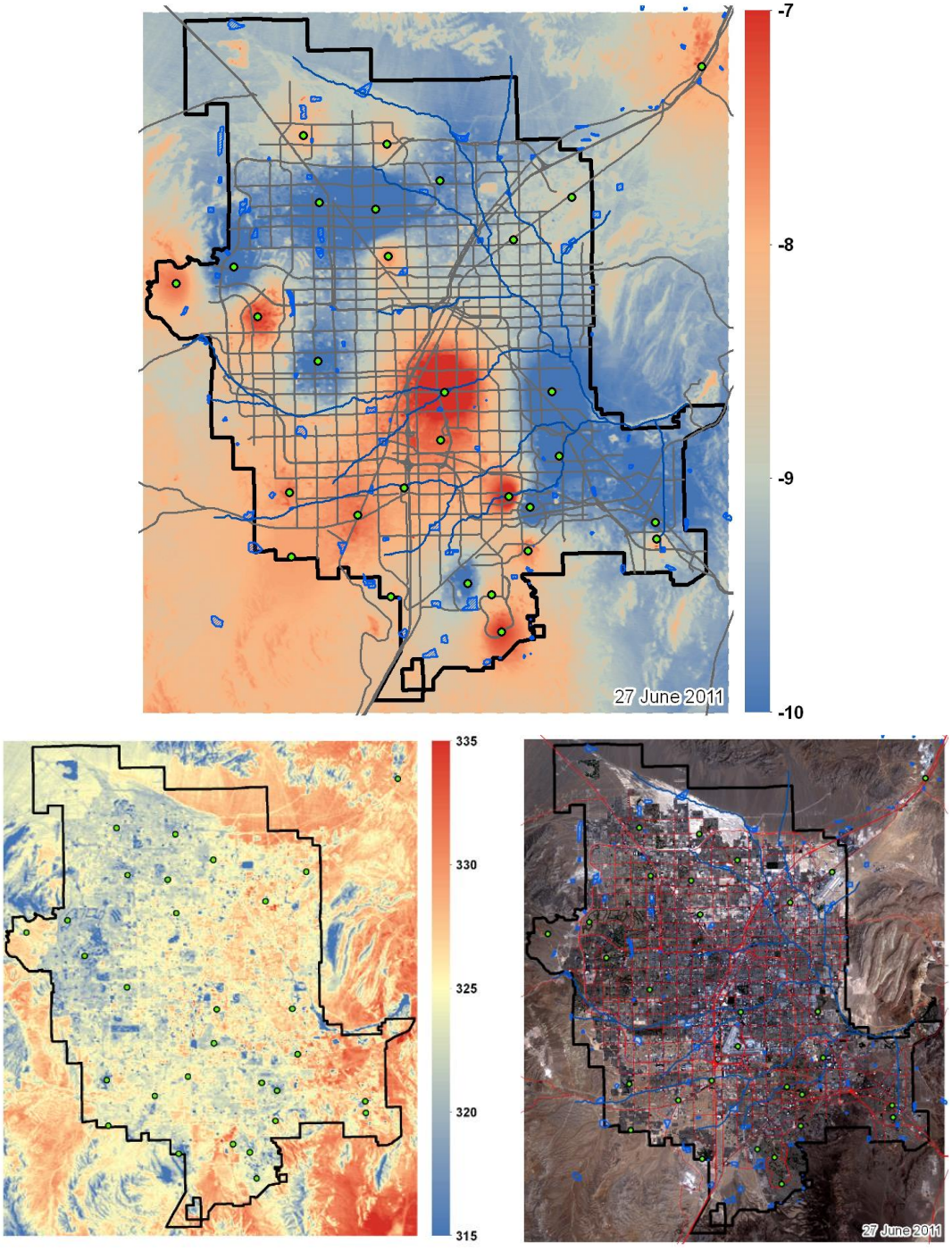

Figure 15. Urban Heat Island Intensity map of Las Vegas (top) on June 27, 2011. Land surface temperature at 10:00 AM (bottom left) and Landsat 5 true color composite image (bottom right) are also shown.

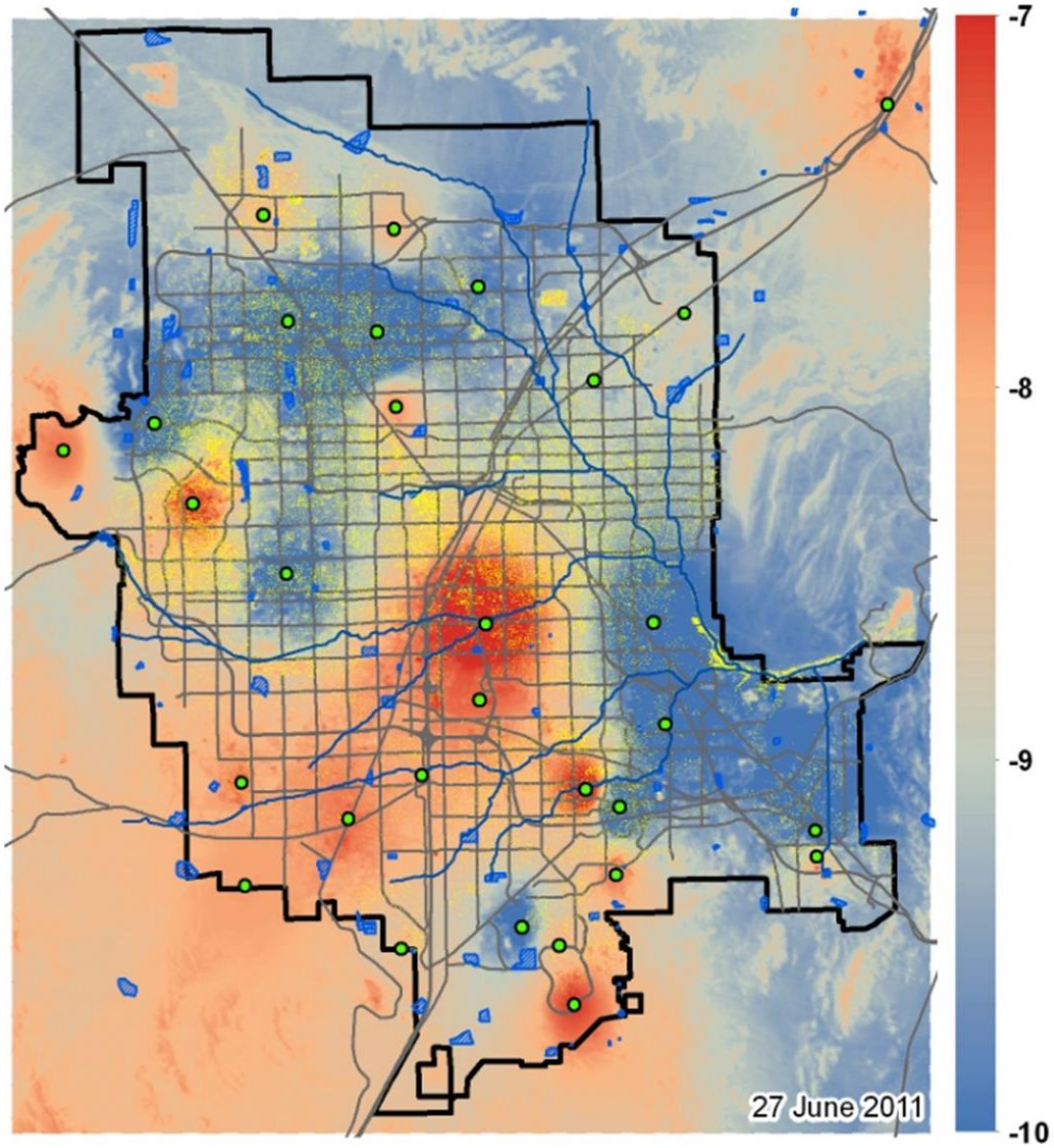

Figure 16. Urban Heat Island Intensity map of Las Vegas on June 27, 2011 overlayed with tree canopy data.

UHII values below -8.5 are mainly located in the City of Las Vegas and northeast City of Henderson districts. These regions correspond to dense residential developments with several dark green color swatches in the true color image that are usually associated with high water maintenance plants.

Figure 16 shows the UHII map with an overlay of the 2006 tree canopy cover data provided by the Southern Nevada Water Authority (*Brandt, 2008*). It is noted that UHII transitions from low to high as tree canopy density is reduced. Examples of this can be observed at the Aliante and North Las Vegas weather stations. The tree line also borders the southwest Las Vegas Valley region where low temperature variation is most likely to occur.

There are some areas that have dense tree canopies in the areas showing UHII greater than negative 8. Noticeable areas include the Angel Park NV US Las Vegas and Elkhorn Springs weather stations located in the northwest valley area. There is also dense vegetation located in the central study area around the Las Vegas US CEMP weather station. Low UHII values were expected to be found in these areas. A possible explanation for these contradictory occurrences is that the presence of dense foliage and trees in urban areas reduce the maximum daytime temperature in that region. Therefore, less energy loss is required to attain rural nighttime temperatures which results in a high UHII value. Additional analysis should be considered to refine the process to distinguish between UHI and cool islands.

In order to further confirm the relation of UHII with tree canopy, we compare high resolution landuse information from NAIP imagery with computed UHII within 500m of selected stations. Figure 17 examines the UHII value increase between three residential communites. These areas are the locations of Sun City Anthem, Elkhorn Springs, and NW Spring Valley weather stations. UHII values in these increase from NW Spring Valley to Elkhorn Springs to Sun City Anthem. Examination of the true color composite images suggests NW Spring Valley has the highest vegetation density while Sun City Anthem has the least plant area. This confirms that UHII increases as plant coverage decreases. Figure 16 shows similar comparison over Weather Dog House and Arden NV US UPR meteorological stations with contrasting urban build-up. The Weather Dog House meteorological station is located in a dense residential region in the City of Las Vegas. The UHII map in this area shows that there is significant temperature cooling within this region. The Arden NV US UPR station is located in the southwest region of the study area where low urbanization has occurred and has high UHII. Comparison of the Weather Dog House and Arden NV US UPR stations shows that in the arid Las Vegas UHII decreases as land development increases.

Above examination of five selected stations indicates that Las Vegas areas where new urban development took place result in lower temperatures while in general, increased vegetation lower UHII. This implies that UHI are more likely to form in areas with little or no vegetation whereas when new development takes place in an arid area it results in an overall cooling effect.

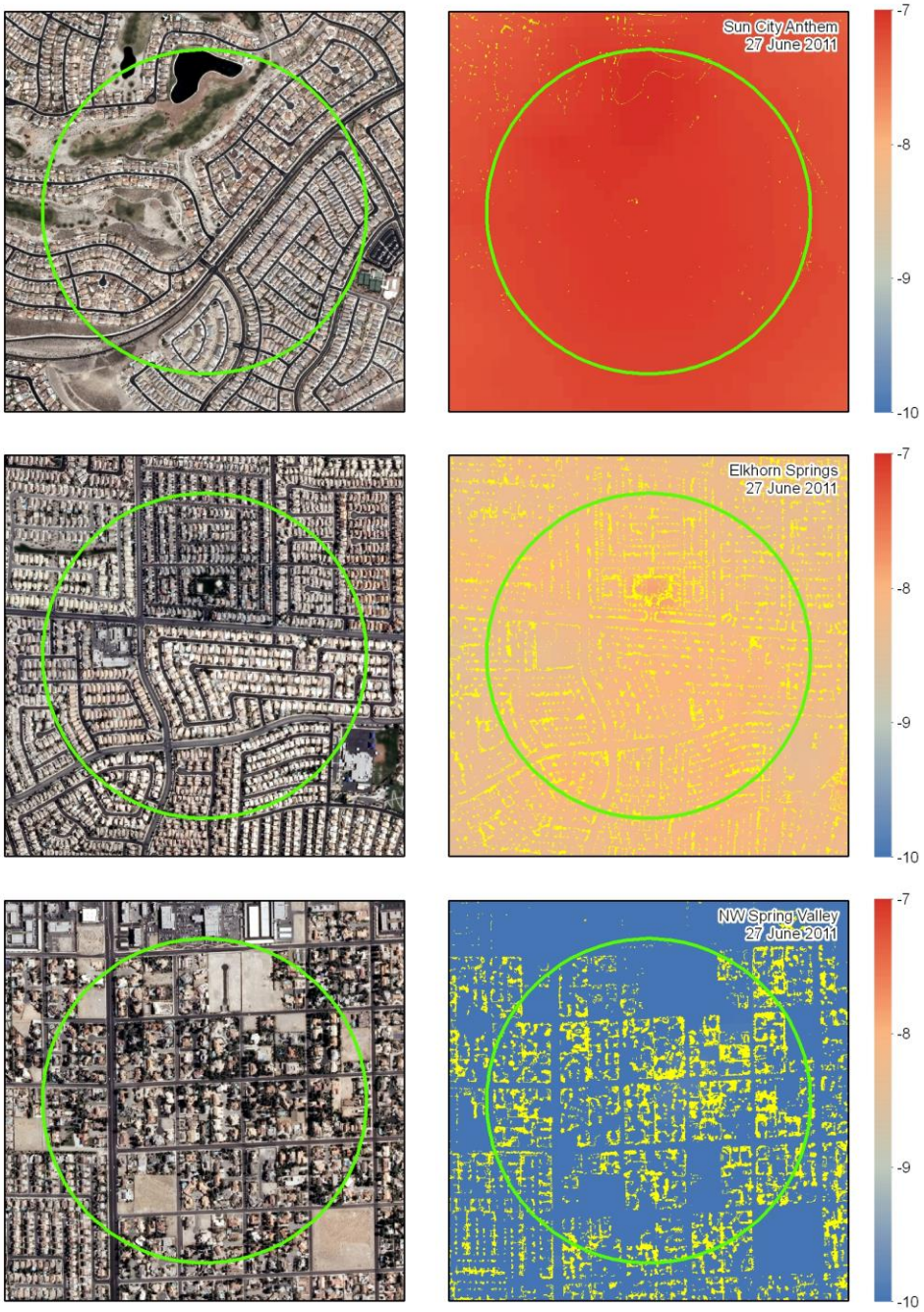

Figure 17. (Left) Urban Heat Island Intensity map of Las Vegas. (Right) Landsat 5 true color composite image.

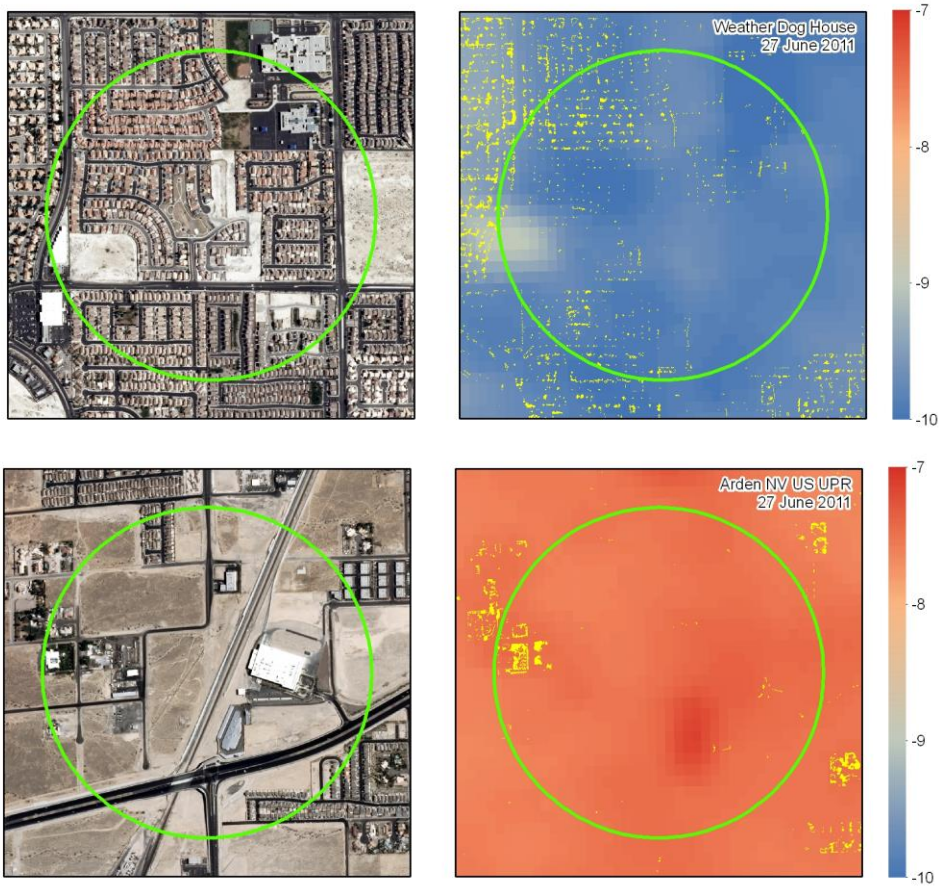

Figure 18. (Left) Urban Heat Island Intensity map of Las Vegas. (Right) Landsat 5 true color composite image.

7 Las Vegas Valley Integrated Zone Map

In order to understand how the UHII is related to various zones of Las Vegas, and integrated landuse map was created by combing the planed landuse maps of all areas acquired from GISMO. The process used to create the Las Vegas zoning map is described below. The zoning map was prepared by merging the landuse maps of the individual cities. In the merging process, careful attention was given to the merging of the different classification schemes used by the cities.

The zoning definitions contained in the building codes are grouped into residential, commercial, industrial, public facilities, open lands, and right of way categories. Any map types not designated within the building codes are classified based on best judgment. A combined table was created as shown in the appendix C.

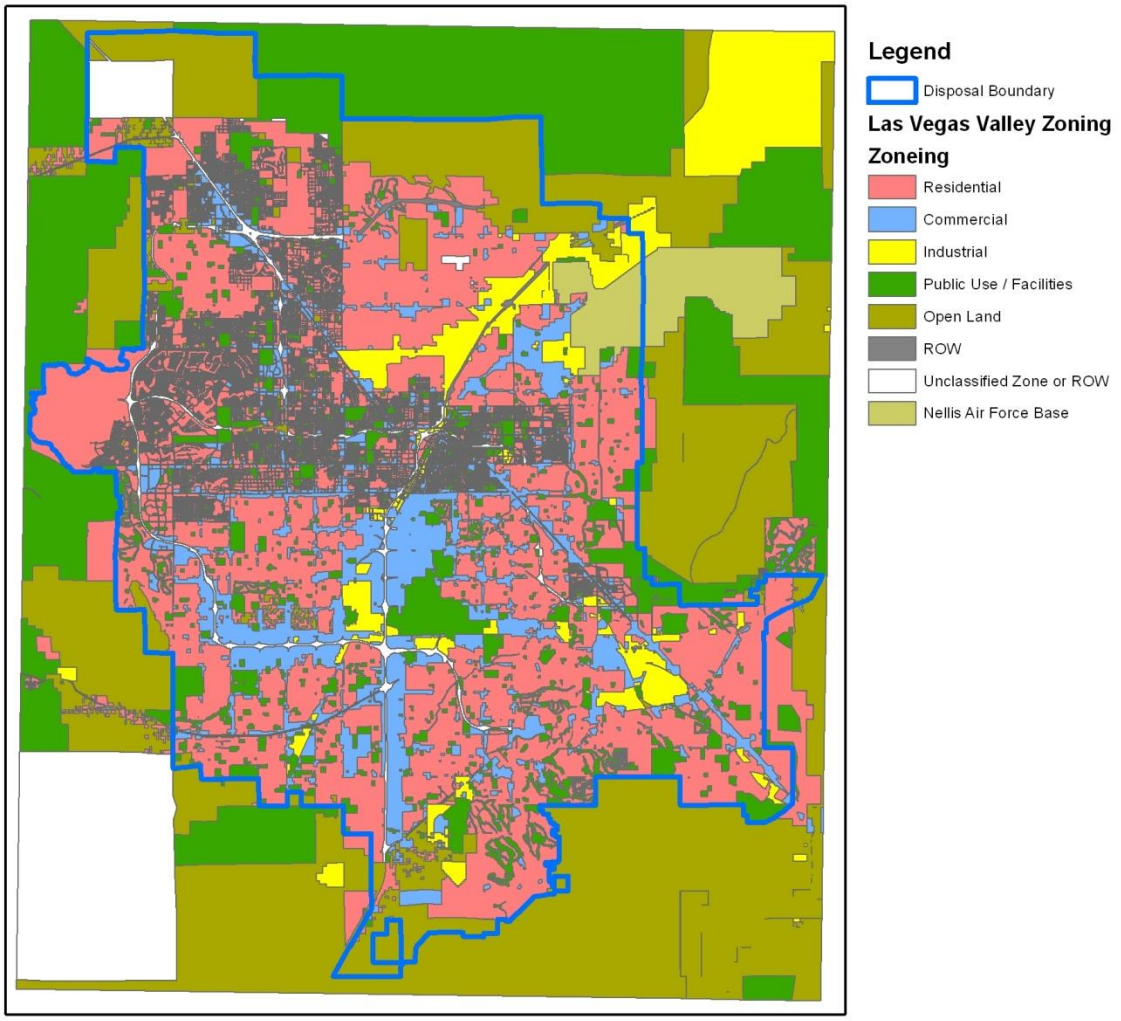

Figure 19. Unified landuse map of Las Vegas.

Shapefiles downloaded from GISMO were opened in ArcMap map document. The attribute tables were then compared to zone map PDF's for accuracy. Shapefiles that matched the PDF's the best were selected to build the valley wide planned land use shapefile. The polygons in each shapefile were exported into separate files based on their zone classification. A column labeled 'ZONE_CODE' was added to each attribute table of the exported shapefiles and populated depending on the shapefile zone classification. There were no agricultural (B6) areas identified in the Las Vegas valley study area.

Below is the list of zones in the combined landuse map.

AFB – Nellis Air Force Base

B1 – Residential
B2 – Commercial
B3 – Industrial
B4 – Public Use / Facilities
B5 – Open Land
B6 – Agricultural
B7 – Right of Way (ROW)
UZ – Unclassified Zone or ROW

All exported files are then combined (merged) into a single file and then clipped to the masking boundary. In the final step, union of zoning shapefile and masking boundary was performed to fill in the unclassified areas. Data was cleaned up by removing the extra columns from the shapefile. The final map is shown in Figure 18. The average value of trends and UHII were calculated for each landuse and the results are tabulated in following Table. Clearly, industrial and commercial areas have highest UHII with trends of -0.072 K/year and -0.066 K/year.

Mean change in temperature by zone type

No.	Zone	Zone Code	Mean	
			UHII	Residual
1	Nellis AFB	AFB	-8.980	-0.028
2	Residential	B1	-8.962	-0.086
3	Commercial	B2	-8.529	-0.083
4	Industrial	B3	-8.644	-0.072
5	Public Use / Facilities	B4	-8.876	-0.066
6	Open Land	B5	-8.879	-0.124
7	ROW	B7	-9.120	-0.077
8	Unclassified	UZ	-8.537	-0.082

8 Summary and Conclusions

The metropolis of Las Vegas has witnessed fast urban growth in the last few decades. This has resulted in modification of geophysical processes including the thermal response of the urban landscape resulting in urban heat island effect. This study is conducted to understand the thermal behavior of Las Vegas by analyzing the temporal response of observed temperature. The results of the study will facilitate in tree planting efforts to reduce the urban heat island effect. Observed

temperature data from ground based meteorological stations and satellite based data remote sensing thermal infrared images are used. Two approaches are followed to perform the study including the trend analysis of temperature time series data from ground based meteorological stations and spatial urban heat island intensity mapping using remote sensing data.

The trend analysis of the point based data is based on the slope of the residual temperature computed by subtracting the average annual response from the data. It shows a general decrease in temperature in most of the central Las Vegas area where as increase at the airport and in the industrial area. The interpolated map provided limited information about the spatial behavior of the trends but can be useful in case of limited spatial sampling. Similar trend analysis of LandSat TM temperature images shows that the old city has experienced increased temperature during the last two decades whereas new development in Las Vegas city has sustained and in some cases experienced negative temperature trends.

Urban heat island intensity (UHII) map is created by subtracting noon air temperature from the midnight air temperature. The images of midnight and noon temperature are created by developing relationships between the remote sensing and ground based temperature data. High UHII values indicate potential urban heat island and are observed at the airport and in the industrial areas.

9 References

Arnfield, A. J. (2003). Two decades of urban climate research: a review of turbulence, exchanges of energy and water, and the urban heat island. International Journal of Climatology, 23(1), 1-26.

Bornstein, R. (2009, January). Tim Oke and the extension of urban heat island observations upwards into the PBL. In Eighth Symposium on the Urban Environment.

Brandt, J. (2008). Locating turf and water features in the Las Vegas valley, Nevada, using remote sensing techniques and GIS. Pecora 17 – The Future of Land Imaging…Going Operational, November 18-20, 2008, Denver, Colorado.

Carlowicz, M. (2009). Ecosystem, Vegetation Affect Intensity of Urban Heat Island Effect. NASA's Earth Science News Team.

Chen, F., Kusaka, H., Bornstein, R., Ching, J., Grimmond, C. S. B., Grossman-Clarke, S., Loridan, T., Manning, K. W., Martilli, A., Miao, S., Sailor, D., Salamanca, F. P., Taha, H., Tewari, M., Wang, X., Wyszogrodzki, A. A. and Zhang, C. (2011), The integrated WRF/urban

modelling system: development, evaluation, and applications to urban environmental problems. Int. J. Climatol., 31: 273–288. doi: 10.1002/joc.2158

Chen, X. L., Zhao, H. M., Li, P. X., and Yin, Z. Y. (2006). Remote sensing image-based analysis of the relationship between urban heat island and land use/cover changes. Remote Sensing of Environment, 104(2), 133-146.

City Council Report. (2010). Population Element: Las Vegas Master Plan 2020.

Comprehensive planning demographics. Retrieved from http://www.clarkcountynv.gov/depts/comprehensive_planning/demographics/documents/historicalcclvvaveragepopgrowthrate.xls

Emmanuel, R., & Kruger, E. (2012). Urban heat island and its impact on climate change resilience in a shrinking city: The case of glasgow, UK. *Building and Environment, 53*, 137-149. doi: 10.1016/j.buildenv.2012.01.020

Frumkin, H. (2002). Urban sprawl and public health. Public health reports, 117(3), 201.

Geller, T. (2007). Envisioning the wind: Meteorology graphics at weather underground. *IEEE Computer Graphics and Applications*, *27*(5), 92-97. doi: 10.1109/MCG.2007.124

Geographic Information Services (GIS). Retrieved Sept. 7, 2012, from <http://www.cityofhenderson.com/gis/index.php>.

Geographic Information System Management Office. Retrieved Sept. 7, 2012, from http://www.clarkcountynv.gov/depts/ccgis/pages/default.aspxGuhathakurta, S., and Gober, P. (2007). The impact of the Phoenix urban heat island on residential water use. Journal of the American Planning Association, 73(3), 317-329.

Grimmond, C. S. B., and Oke, T. R. (2002). Turbulent heat fluxes in urban areas: Observations and a local-scale urban meteorological parameterization scheme (LUMPS). Journal of Applied Meteorology, 41(7), 792-810.

Imhoff, M. L., Zhang, P., Wolfe, R. E., and Bounoua, L. (2010). Remote sensing of the urban heat island effect across biomes in the continental USA. Remote Sensing of Environment, 114(3), 504-513.

Kolokotroni, M., Giannitsaris, I., and Watkins, R. (2006). The effect of the London urban heat island on building summer cooling demand and night ventilation strategies. Solar Energy, 80(4), 383-392.

McCarthy, M. P., Best, M. J., and Betts, R. A. (2010). Climate change in cities due to global warming and urban effects. Geophysical Research Letters, 37(9), L09705.

Oke, T. R. (1973). City size and the urban heat island. Atmospheric Environment (1967), 7(8), 769-779.

Oke, T. R. (1976). The distinction between canopy and boundary-layer urban heat islands. Atmosphere, 14(4), 268-277.

Remar, A. (2010). Urban Heat Island Expansion in the Greater Las Vegas Metropolitan Area.

Rosenzweig, C., Solecki, W. D., Parshall, L., Chopping, M., Pope, G., & Goldberg, R. (2005). Characterizing the urban heat island in current and future climates in New Jersey. Global Environmental Change Part B: Environmental Hazards, 6(1), 51-62.

Sherman-Morris, K., Senkbeil, J., & Carver, R. (2011). Who's googling what? what internet searches reveal about hurricane information seeking. *Bulletin of the American Meteorological Society, 92*(8), 975-985. doi: 10.1175/2011BAMS3053.1

USGS global visualization viewer. Retrieved Aug. 12, 2012, from http://glovis.usgs.gov/index.shtml

Voogt, J. A., and Oke, T. R. (2003). Thermal remote sensing of urban climates. Remote sensing of Environment, 86(3), 370-384.

Xian, G., and Crane, M. (2006). An analysis of urban thermal characteristics and associated land cover in Tampa Bay and Las Vegas using Landsat satellite data. Remote Sensing of Environment, 104(2), 147-156.

Xian, G. (2008). Satellite remotely-sensed land surface parameters and their climatic effects for three metropolitan regions. *Advances in Space Research, 41*(11), 1861-1869. doi: 10.1016/j.asr.2007.11.004

Wilby, R. L. (2003). Past and projected trends in London's urban heat island. Weather, 58(7), 251-260.

Wundermap. Retrieved 08 February, 2013, from http://www.wunderground.com/wundermap/

WunderWiki main page. Retrieved 08 February, 2013, from http://wiki.wunderground.com/index.php/Main_Page

Zhang, X., Zhang, M., Zhang, J., & Yang, Y. (2011). Spatial correlation analysis between impervious surface, green space and urban heat island. Paper presented at the *2011 19th International Conference on Geoinformatics, Geoinformatics 2011, June 24, 2011 - June 26,* IEEE Geoscience and Remote Sensing Society (IEEE GRSS); East China Norm. Univ., Sch. Resour. Environ. Sci.; Shanghai Urban Dev. Inf. Res. Cent.; The Geographical Society of Shanghai; East China Univ. Sci. Technol., Bus. Sch. doi: 10.1109/GeoInformatics.2011.5980744.

10 Appendix A: Parameters of the trend analysis of the residual temperature time series

No	Station Name	Station ID	Start Year	End Year	Slope (K/yr)
1	Henderson Executive Airport	KHND	2002	2012	-0.320
2	McCarran Airport	KLAS	1948	2012	0.041
3	Nellis AFB	KLSV	1942	2012	0.020
4	Seven Hills	KNVHENDE12	2006	2011	-0.179
5	MacDonald Ranch	KNVHENDE15	2006	2011	-0.302
6	Bailes Home Weather	KNVHENDE16	2009	2011	-0.132
7	Sun City Anthem	KNVHENDE17	2006	2011	-0.330
8	Whitney Ranch-Residential	KNVHENDE22	2009	2011	0.066
9	Legacy Golf Course Area	KNVHENDE6	2004	2011	-0.021
10	Rhodes Ranch	KNVLASVE11	2002	2011	-0.015
11	Photo Patterns	KNVLASVE23	2004	2011	-0.121
12	Neon Desert Weather, East Las Vegas	KNVLASVE25	2004	2011	-0.029
13	NW Spring Valley	KNVLASVE32	2005	2011	-0.102
14	Photo Patterns	KNVLASVE35	2005	2011	0.076
15	Centennial Hills	KNVLASVE54	2008	2011	-0.283
16	Southern Highlands	KNVLASVE57	2010	2011	-0.301
17	Elkhorn Springs	KNVLASVE8	2009	2011	-0.483
18	Palomino Estates	KNVNORTH1	2001	2011	-0.106
19	Weather Dog House	KNVNORTH6	2009	2011	-0.404
20	Aliante	KNVNORTH8	2009	2011	-0.087
21	North Las Vegas Airport	KVGT	1997	2012	-0.077
22	Angel Park NV US Las Vegas	MAPWN2	2007	2011	-0.091
23	Henderson NV US	MC7282	2007	2011	-0.425
24	Henderson NV US CEMP	MCMP10	2007	2011	-0.202
25	Las Vegas NV US CEMP	MCMP12	2007	2011	-0.258
26	Las Vegas NV US CEMP	MD5026	2010	2011	-0.532
27	Las Vegas NV US	MD5799	2010	2011	-0.160
28	Summerlin West NV US Las Vegas	MSMWN2	2010	2011	0.312
29	Apex NV US UPR	MUP052	2009	2011	-0.480
30	Arden NV US UPR	MUP076	2007	2011	-0.216

11 Appendix B: Parameters of the Midnight and Noon Air Temperature Models

11.1 Midnight Air Temperature Model Regression and Correlation Parameters

No	Station Name	StationID	Slope (m)	Intercept (b)	Correlation	RMSE	p-Value
1	Henderson Exec. Airport	KHND	0.688	79.9	0.827	6.694	0
2	McCarran Airport	KLAS	0.736	68.5	0.848	6.309	0
3	Nellis AFB	KLSV	0.620	103.2	0.771	6.366	0
4	Seven Hills	KNVHENDE12	0.720	72.0	0.881	9.233	0
5	MacDonald Ranch	KNVHENDE15	0.712	73.4	0.926	9.427	0
6	Bailes Home Weather	KNVHENDE16	0.709	75.5	0.822	10.094	0
7	Sun City Anthem	KNVHENDE17	0.751	62.1	0.939	9.380	0
8	Whitney Ranch	KNVHENDE22	0.778	53.4	0.961	9.815	0
9	Legacy Golf Course Area	KNVHENDE6	0.760	61.5	0.946	8.922	0
10	Rhodes Ranch	KNVLASVE11	0.812	45.4	0.932	8.961	0
11	Photo Patterns	KNVLASVE23	0.681	83.1	0.939	9.217	0
12	Neon Desert Weather	KNVLASVE25	0.734	65.5	0.930	9.809	0
13	NW Spring Valley	KNVLASVE32	0.649	94.2	0.937	7.920	0
14	Photo Patterns	KNVLASVE35	0.684	82.2	0.918	8.370	0
15	Centennial Hills	KNVLASVE54	0.560	120.0	0.861	7.939	0
16	Southern Highlands	KNVLASVE57	0.758	63.3	0.964	9.974	0
17	Elkhorn Springs	KNVLASVE8	0.624	101.4	0.915	8.552	0
18	Palomino Estates	KNVNORTH1	0.595	108.7	0.864	8.342	0
19	Weather Dog House	KNVNORTH6	0.628	99.6	0.889	8.772	0
20	Aliante	KNVNORTH8	0.683	82.7	0.896	9.275	0
21	North Las Vegas Airport	KVGT	0.742	65.4	0.841	6.351	0
22	Angel Park	MAPWN2	0.738	67.2	0.930	8.638	0
23	Henderson NV US	MC7282	0.804	46.1	0.931	8.581	0.000001
24	Henderson NV US CEMP	MCMP10	0.718	71.8	0.928	9.585	0
25	Las Vegas NV US CEMP	MCMP12	0.745	65.5	0.938	9.386	0
26	Las Vegas NV US CEMP	MD5026	0.775	53.6	0.927	9.907	0
27	Las Vegas NV US	MD5799	0.801	46.5	0.955	10.731	0
28	Summerlin West	MSMWN2	0.718	71.8	0.884	10.051	0.000001
29	Apex NV US UPR	MUP052	0.641	94.5	0.929	8.871	0
30	Arden NV US UPR	MUP076	0.656	91.1	0.948	8.122	0

11.2 Noon Air Temperature Model Regression and Correlation Parameters

No	Station Name	StationID	Slope (A_n)	Intercept (B_n)	Correlation	RMSE	p-Value
1	Henderson Exec. Airport	KHND	0.772	62.9	0.938	10.0	0
2	McCarran Airport	KLAS	0.777	62.6	0.943	9.9	0
3	Nellis AFB	KLSV	0.699	86.2	0.919	9.7	0
4	Seven Hills	KNVHENDE12	0.758	67.9	0.906	9.5	0
5	MacDonald Ranch	KNVHENDE15	0.734	73.8	0.938	9.4	0
6	Bailes Home Weather	KNVHENDE16	0.816	51.8	0.861	11.1	0
7	Sun City Anthem	KNVHENDE17	0.765	64.9	0.938	9.6	0
8	Whitney Ranch	KNVHENDE22	0.826	48.5	0.948	11.1	0
9	Legacy Golf Course Area	KNVHENDE6	0.910	24.4	0.959	10.5	0
10	Rhodes Ranch	KNVLASVE11	0.852	40.1	0.946	9.3	0
11	Photo Patterns	KNVLASVE23	0.732	75.2	0.944	9.9	0
12	Neon Desert Weather	KNVLASVE25	0.740	74.1	0.939	9.8	0
13	NW Spring Valley	KNVLASVE32	0.768	66.1	0.842	10.7	0
14	Photo Patterns	KNVLASVE35	0.815	50.6	0.954	9.5	0
15	Centennial Hills	KNVLASVE54	0.675	93.4	0.922	8.7	0
16	Southern Highlands	KNVLASVE57	0.808	55.7	0.949	10.8	0
17	Elkhorn Springs	KNVLASVE8	0.714	80.6	0.930	9.6	0
18	Palomino Estates	KNVNORTH1	0.775	63.7	0.946	9.9	0
19	Weather Dog House	KNVNORTH6	0.737	74.1	0.943	9.7	0
20	Aliante	KNVNORTH8	0.677	92.7	0.923	9.0	0
21	North Las Vegas Airport	KVGT	0.756	68.7	0.944	9.9	0
22	Angel Park	MAPWN2	0.785	59.5	0.908	10.1	0
23	Henderson NV US	MC7282	0.791	56.7	0.914	8.5	0
24	Henderson NV US CEMP	MCMP10	0.794	54.9	0.936	10.2	0
25	Las Vegas NV US CEMP	MCMP12	0.759	66.7	0.929	9.5	0
26	Las Vegas NV US CEMP	MD5026	0.760	66.5	0.917	9.8	0
27	Las Vegas NV US	MD5799	0.812	51.1	0.954	10.9	0
28	Summerlin West	MSMWN2	0.734	74.1	0.930	9.8	0
29	Apex NV US UPR	MUP052	0.685	88.0	0.941	9.5	0
30	Arden NV US UPR	MUP076	0.697	85.2	0.943	8.6	0

12 Appendix C: Merged PLU Table of Las Vegas

City of Las Vegas		City of North Las Vegas		City of Henderson		Boulder City		Clark County		Summerlin South		Reclassification	
Zone Designation	Zone	Zone Designation	Zone	Zone Designation	Code	Designation	Class	Designation	PLU	Designation	PLU	Label	Code
Ranch Acres	R-A	Ranch Estates District	R-E	Low-Density Single-Family Residential 1	RS-1	Single-family residential zone	R1	Residential Countryside	RC	Single Family	SF	Residential	B1
Residential Estates	R-E	Ranch Estates Limited District	R-EL	Low-Density Single-Family Residential 2	RS-2	Two-family residential zone	R2	Residential Rural	RR	Multi-Family	MF		
Single-Family Residential Restricted	R-O	Single-Family Low Density District	R-1	Low-Density Single-Family Residential 4	RS-4	Multiple-family residential zone	R3	Residential Agricultural	RA				
Residential Planned Development	R-PD1	Single-Family Medium Density District	R-2	Low-Density Single-Family Residential 6	RS-6	Mobile home park zone	MP	Rural Neighborhood	RN				
	R-PD2	Multi-Family Residential District	R-3	Low-Density Single-Family Residential 8	RS-8	Mobile home estate zone	ME	Rural Neighborhood Preservation	RNP				
	R-PD3	High Density Residential District	R-4	Medium-Density Residential 10	RM-10	Recreational vehicle zone	RV	Residential Low	RL				
	R-PD4	Medium Density Residential Subdistrict	R-A/R-2	Medium-Density Residential 16	RM-16	Planned unit development	PUD	Residential Suburban	RS				
	R-PD5	Single-Family Compact Lot Residential Subdistrict	R-2/R-3	High-Density Multi-Family Residential 24	RH-24	Senior housing zone	SH	Residential Medium	RM				
	R-PD6	Single-Family Compact Lot Residential District	R-C	High-Density Multi-Family Residential 36	RH-36			Residential High	RH				
	R-PD7	Planned Unit Development District	PUD	Downtown Low-Density Residential	DRL			Residential Urban Center	RUC				
	R-PD8	Focus Area	R-A/FA	Downtown Medium-Density Residential	DRM			Residential High Rise Center	RHRC				
	R-PD9	Master Planned Community	MPC	Downtown High-Density Residential	DRH			Major Development Projects	MDP				
	R-PD10		MPC R-1	Mobile/Manufactured Home Residential	RMH			Mixed Use PUD	MIX				
	R-PD11		MPC R-3	Development Holding	DH								
	R-PD12		MPC PUD	Planned Community	PC								
	R-PD13 to R-PD46												
Single Family Residential	R-1												
Medium-Low Density Residential	R-2												
Medium Density Residential	R-3												
High Density Residential	R-4												
Apartment	R-5												
Mobile/Manufactured Home	R-MH												
Single Family Compact-Lot	R-CL												
Residential Mobile/Manufacture Home Park	R-MHP												
Planned Community	P-C												
Planned Development	PD												
Traditional Development	T-D												
Professional Office	P-R	Commercial/Retail	R-A/CR	Neighborhood Commercial	CN	Special Recreation Zone	SR	Office Professional	OP		GC	Commercial	B2
Neighborhood Services	N-S	Gaming/Hotel/Entertainment	R-A/CHE	Office Commercial	CO	Neighborhood commercial zone	C1	Commercial Neighborhood	CN	Casino	C		
Office	O	Office	R-A/OFFICE	Community Commercial	CC	General commercial zone	C2	Commercial General	CG	Residential/Commercial	RC		
Designed Commercial	C-D	Neighborhood Commercial District	C-1	Highway Commercial	CH	Central business district	CBD	Commercial Tourist	CT	Commercial/Church	CC		
Limited Commercial	C-L	Limited Commercial District	C-2	Limited Commercial	CL	Business and office park	BOP	Business and Design/Research Park	BNP				
General Commercial	C-2	General Service Commercial District	C-3	General Commercial	GC	Commercial manufacturing zone	CM	Commercial Industrial	CI				
Commercial/Industrial	C-M	Professional Office Commercial District	C-P	Downtown Core Commercial	DCC								
Planned Business Park	C-PB		MPC C-1	Downtown Highway Commercial	DHC								
Town Center	T-C		MPC C-2	Corridor / Community Mixed-Use	MC								
			MPC C-P	Regional Mixed-Use	MR								
Industrial	M	Business Park Industrial District	M-1	Limited Industrial	IL	Energy resource zone	ER	Industrial	IND			Industrial	B3
		General Industrial District	M-2	General Industrial	IG			Heavy Industrial	HI				
		Heavy Industrial District	M-3	Industrial Park	IP			Mineral Extraction	ME				
Civic	C-V	Public/Semi-Public District	PSP	Downtown Public	DP	Hospital zone	H	Public Facilities	PF	Public Facility	PF	Public Use	B4
			MPC PSP	Public and Semipublic	PS	Parks/Recreation	GP	Parks and Recreation	PR	Park/Open Space	POS		
			R-A/PSP			Public utilities	GM	Institutional	I				
						Resource-control facilities	GCC		IL				
						Largest zone	AP		P				
						Special agricultural zone	A-1	Agricultural	AG			Agricultural	B6
						Corral zone	CO						
Undeveloped	U(DR)	Open Land District	O-L	County	CNTY	Interim study zone	S	Open Lands	OL	Steep Slopes	S	Open Space	B5
	U(L)		O-L/DA			Open space	GO						
	U(L)/A						OS						
	U(M)												
	U(M1)												
	U(O)												
	U(PCD)												
	U(PF)												
	U(RDS)												
	U(R)												
	U(RE)												
	U(RE)												
	U(RNP)												
	U(ROW)												
	U(SC)												
	U(TC)												
	U(TND)												
			PUBLIC ROW					Right of Way	ROW			Public ROW	B7
			FWY										